DEFLECTION ANALYSIS IN BEAMS REINFORCED WITH GFRP

Davi Pitangui P. Abreu[1] Arthur Francisco Claro Ribeiro[1] Antonio P. Peruzzi[1] Rodrigo Gustavo Delalibera[1]
[1]Department of Civil Engineering, Universidade Federal de Uberlandia, Uberlandia, MG, 38.400-902, Brazil
davipitanguiabreu@gmail.com, arthribeiro@ufu.br aperuzzi@ufu.br, delalibera@ufu.br

ABSTRACT

Fiber-reinforced polymer composites utilizing glass fibers (GFRP) represent an established solution for concrete reinforcement, particularly in corrosive settings or applications requiring non-magnetic properties. Unlike conventional steel reinforcement, GFRP rebars are not subject to corrosion, which translate into an increased service life of structural members in harsh environments such as marine atmospheres, industrial plants or infrastructures influenced by de-icing salts. In the same study, a series of test program were done to quantify the mechanical properties of GFRP bars, in terms of effective-diameter, tensile strength and modulus of elasticity. Then three types of beams were compared and studied; one with a conventional deformed steel as strengthening method, the second one used FRP bars to serve as a "super-reinforced" beam and a third design was made for the optimized shapes in section geometry increasing the moment of inertia performance using GFRP bars for reinforcement. It was showed by the experimental and analytical results that beam with GFRP as a reinforcement has fulfilled satisfactory structural performance. Then, the optimal geometry as well as the super-reinforced beam attained comparable stiffness to that of the steel-reinforced reference beam. It is also apparent from the results that substitution of traditional reinforcement with GFRP can be technically feasible. On the other hand, if geometrical optimization of the structural member is possible, higher inerialicity may be safely considered as a cost-effective measure since it merges together structural adequacy and economy.

KEYWORDS: *GFRP; Durability; Fiber Concrete; Composites*

I. INTRODUCTION

The durability of reinforced structures depends on materials that are not corroded by aggressive agents. When analyzing alternative metal-reinforced materials, GFRP (glass fiber reinforced polymer) stands out for its technical and economic advantages compared to stainless steel, for example, which has high mechanical strength, durability in aggressive environments, lightness, and "magnetic transparency" [1]. Although GFRP has high Tensile Strength (about 1,000 MPa), when analyzing the structural design, the use of GFRP represents important changes in the reinforced concrete beams mainly its significantly lower modulus of elasticity, as noted in the abstract, leads to excessive deformations, then the design of structural with GFRP is typically governed by Serviceability Limit States, in particular Deflection Criteria. In this study, were proposed two different ways to get around the excessive deformations: 1st) using E_{GFRP} as limit for the calculation, resulting in bigger quantity of GFRP bars (classical procedure, but resulting in more expensive structures) (beam type **B2**), and 2nd increasing the inertia of the structural element (increasing them beam height) (beam type **B3**), both compared with a reinforced beam with steel bars (as reference) (beam type **B1**).

The simply supported beams were designed in reinforced concrete with GRP bars as reinforcement based on the guidelines of ACI 440.1R [2], and this analysis included the evaluation of two distinct types of deflections: instantaneous (immediately after the load is applied) and final (which considers long-term effects, such as concrete creep). The Deflection Calculation models proposed in the literature

and their applicability to beams reinforced with GFRP were also discussed, comparing the theoretical results with the Four-point bending tests performed.

This paper is organized in the following manner: Section II presents the methodology employed; results and discussion are presented in Section III and the main conclusions drawn from the study are presented in Section IV.

II. METHODOLOGY

2.1. Characterization of the bars

GFRP bars were characterized regarding Effective diameter, Tensile Strength ($\mathbf{f_t}$), and Elasticity Modulus (**E**) carried out as [3]. To determine the effective diameter, five bars, each with a minimum mass of 50 g, were randomly selected from a 100-meter length. The Effective diameter (ϕ_{ef}) was calculated as Equation 1.

$$\phi_{ef} = \sqrt{\frac{4 \times (m_1 - m_2)}{\pi \times \rho \times l}} \quad \text{(Eq. 1)}$$

where:
m_1: apparent mass of the sample (air) (kg)
m_2: apparent mass of the sample immersed in water (in hydrostatic balance) (kg)
ρ: density of water, assumed as 1 kg/m³
l: average length of the samples (m)

For the $\mathbf{f_t}$ and **E** determination was necessary to prepare samples whose ends received metal pipes filled with epoxy resin (as Figure 1a and 1b). This procedure aims to ensure that the bars do not break up in the clutches of the machine due to Crushing of the section (as Figure 1c). Equation 2 and Equation 3 brings the $\mathbf{f_t}$ and **E** calculus.

a) **b)** **c)**

Figure 1. Samples prepared for tests of Tensile Strength (f_t), and Elasticity Modulus (E).

$$f_t = \frac{P}{A_{ef}} \quad \text{(Eq. 2)}$$

where:
P: Load max (N)
A_{ef}: Effective area of cross section of the bar (m²)

$$E_f = \frac{(P_1 - P_2)}{(\varepsilon_1 - \varepsilon_2) \times A_{ef}} \quad \text{(Eq. 3)}$$

Where:
P_1: Load with deformation is 0.003 (N)
P_2: Load with deformation is 0.001 (N)
ε_1: specific deformation of 0.003
ε_2: specific deformation de 0.001

Also were tested the bars used in the beam reinforced with steel (**B1**) and those used as stirrups on all beams studied (**B1**, **B2** and **B3**). Tests were conducted on a universal machine EMIC DL60,000 following [4], which aligns with [5]. For each type of bar and diameter, three samples were tested, with the results expressed based on the average values obtained.

2.2. Structural beam design

The dimensioning of the beams was carried out using as Reference a beam reinforced with 2 bars of steel with 10 mm of diameter in the tensile zone, and another 2 bars in the compressed zone, called **B1**. The design of Beam **B2** incorporated 10 mm diameter GFRP bars, utilizing the Elastic Modulus (E) as the governing design parameter. A third beam model called **B3** was developed, using two 10 mm diameter GFRP bars positioned both in the tension and compression zones, with the beam height increased by 5 cm, seeking to increase its rigidity to correct the difference between the E_{GFRP} and E_{steel}. In all beams analysed (**B1**, **B2**, **B3**) was used stirrups of the steel bars with ϕ = 5 mm spaced every 15 cm. Table 1 synthesizes the structural dates used in the beams studied.

Table 1. Structural design dates

Beam	Material	Nº of bars	Φ bar	Dimension (cm)	Length (m)
B1	Steel	2	10	15x30	200
B2	GFRP	6	10	15x30	200
B3	GFRP	2	10	15x35	200

The Resisting Moment was calculated using [2] and [6], next was determined Vertical Deflection in each structural element. To obtain results that were more representative of the real structural capacity, it was decided to disregard the coefficients of reduction of the resistance of the materials (concrete and reinforcement) and the coefficient of increase of the applied actions. Beams reinforced with GFRP was design by [2] and the reinforcement ratio used was lower than the balancing ratio, which defines whether the failure will occur due to the rupture of the concrete or the polymer reinforcement. Equation 4 was used to set this parameter.

$$\rho_{fb} = 0{,}85 \times \beta_1 \times \frac{f_{cm}}{f_{fu}} \times \left(\frac{E_f \times \varepsilon_{cu}}{E_f \times \varepsilon_{cu} + f_{fu}}\right) \quad \text{(Eq. 4)}$$

Where:
β_1 proportion between equivalent compression block depth
f_{cm} concrete compressive tensile average
f_{fu} ultimate bars tensile strength
E_f GFRP bars Elasticity Modulus
ε_{cu} ultimate deflexion of compressed concrete

In order to improve estimates related to the vertical deflection of structures reinforced with GFRP, two different approaches were adopted in relation to deflection:

(1) equivalent stiffness model proposed by Branson

(2) mean curvature obtained experimentally

Branson's model is widely used in stell reinforced concrete and treat a "weighted average effective stiffness" between fissured and non-fissured zone. For the beams reinforced with GFRP this model can be adapted thorough changes suggested by [7] and [8] to represent more precisely the structural response in terms of deflection. Equation 5 calculate the Equivalent Inertia by [9] adapted.

$$I_e = \left(\frac{M_{cr}}{M_a}\right)^3 \times I_g + \left[1 - \left(\frac{M_{cr}}{M_a}\right)^3\right] \times I_{cr} \quad \text{(Eq. 5)}$$

Where:
I_e Equivalent Inertia
M_{cr} Moment of cracking
M_a Acting moment in the section considered

I_g Gross inertia
I_{cr} Moment of inertia at Stage II of cracked section

At the same time, in order to validate the theoretical results, the mean curvature calculation methodology was also used, as recommended by the Canadian Standard [10]. This approach considers the integration of curvature along the beam span, based on three specific displacement measurements taken during the experimental tests – two points close to the supports and one in the middle of the span – allowing the determination of the average curvature radius of the part and, consequently, the corresponding deflection with the greatest approximation to the real behaviour observed in the laboratory. Equation 6 estimate the radius of curvature on the beam from geometry obtained by experiments. Figure 2 shows this process.

$$\frac{1}{R} = \frac{M}{E_{eq} \times I_{eq}} \quad \text{(Eq. 6)}$$

Where:
R Radius estimated by the observed displacements
M Resistant Moment (kN.m)
E_{eq} Equivalent Elasticity Modulus
I_{eq} Equivalent Inertia Modulus

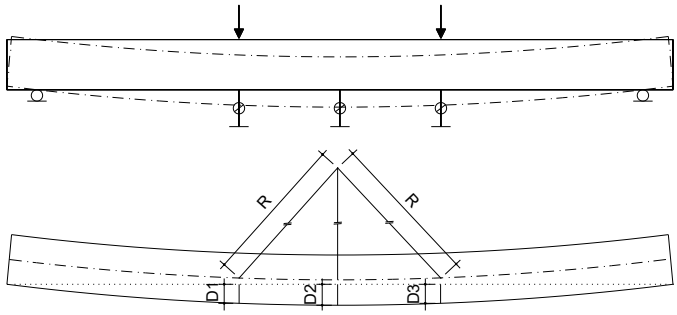

Figure 2. Diagram for obtaining the radius of curvature

To each type of beams two samples were made, so to beam reinforced only with steel (B1) was molded two beams called B1.1 and B1.2 and the same is valid to another types of beams (B2.1 and B2.2, B3.1 and B3.2). The concrete used on the beams was composed of Portland cement, sand, gravel, fiberglass (FG), polypropylene (PP), plasticizer additive and water as described by [11] and its proportions is given by Table 2.

Table 2. Proportions of concrete materials for beam concreting.

Cement (kg/m³)	Sand #2,37 (kg/m³)	Gravel (Basalt) #19,1 (kg/m³)	Fiberglass (kg/m³)	PP (kg/m³)	Water (l)	Plasticizer additive
350.20	810.72	1,071.62	10.05	1.14	192.61	1.62%

The Mold used to make the beams was of wood with dimension 15 x 30 x 200 cm (height x width x length), except **B3** which has dimensions of 5 cm × **35** x 200. Concrete was prepared in loco and compacted by internal concrete vibrator. After the beams was molded, she was submitted to a process of wet cure for 7 days protected by plastic sheets to avoid excessive water loss and good cement hydration. Figure 3 illustrates beams already molded and after being demolded.

Figure 3. Beams in the wood molds, and alteready unmolded.
Search: Authors (2024)

Figure 4a, 4b e 4c detail beam with reinforcement only in stell (**B1**), **B2** reinforced in GFRP (8 bars ϕ = 10 mm) in the longitudinal and steel in the transversal reinforcement (stirrups), and **B3** with reinforcement in GFRP (4 bars ϕ = 10 mm) in the longitudinal and steel as stirrups, but greater height (35mm, against 30mm of **B1** and **B2**). Figure 5 shows beams **B1**, **B2** and **B3** before concreting.

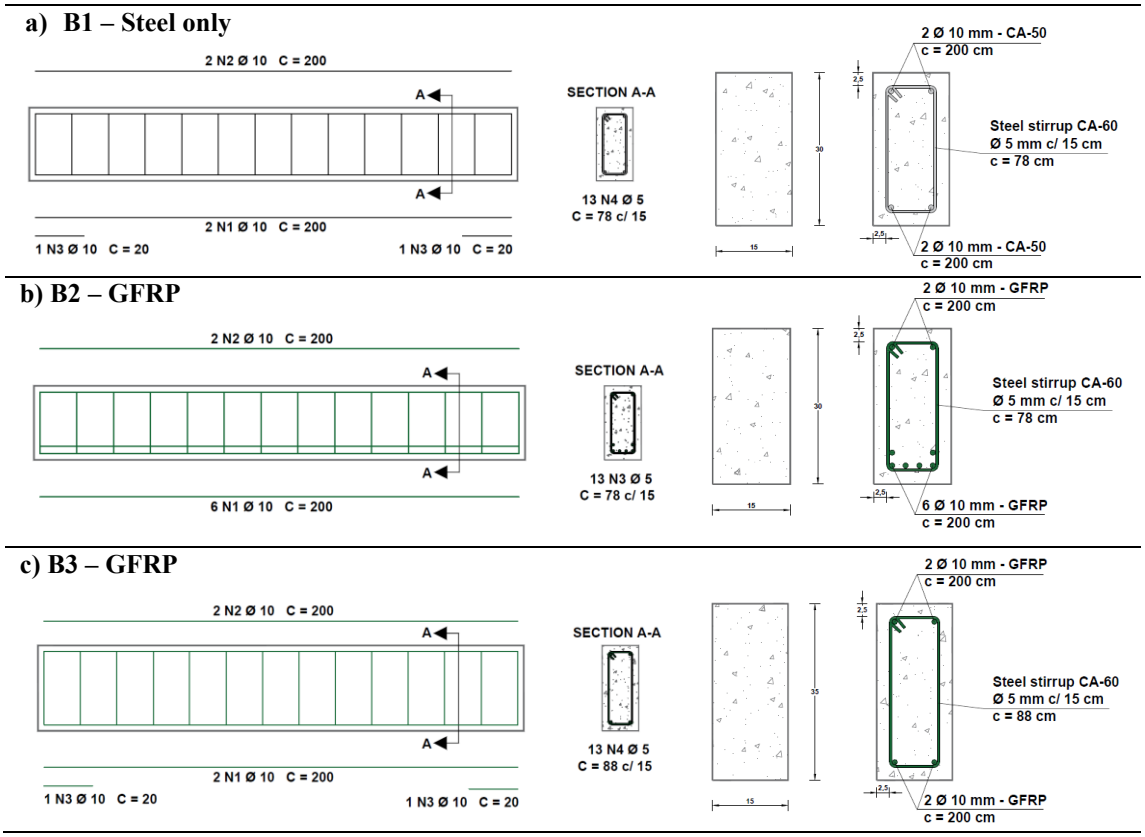

Figure 4. Beam's reinforcement detail and cross section. 4a) **B1** steel only; 4b) **B2** GFRP reinforcement and c) **B3** GFRP reinforcement and greater height. Source: Authors (2024)

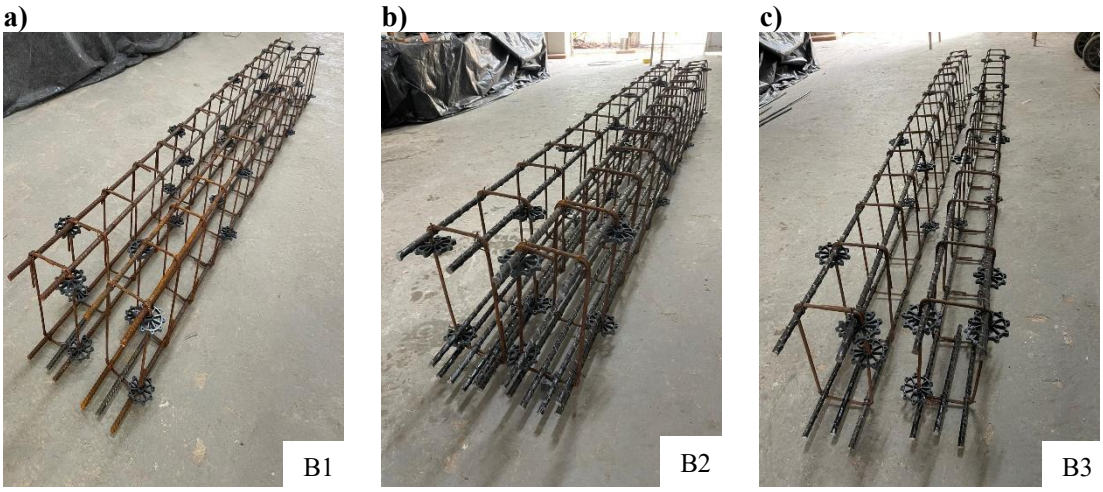

Figure 5. Beam's reinforcement before concreting. 5a. Steel only, 5b and 5c GFRP reinforcement. Source: Authors (2024)

2.4. Flexural test of beams

Flexural test of beams was conducted in accordance with the procedures established by the Standard [12], and Figure 6 shows the experimental model.

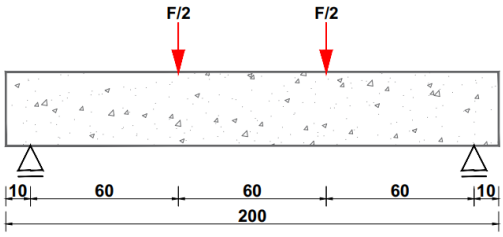

Figure 6. Model of tests used

By the tests was evaluated the experimental parameters:

1) Load and deflection
2) Load ultimate recorded and its rupture displacement by Equation 7

$$f_{ct,f} = \frac{F \times L}{b \times d^2} \quad \text{(Eq. 7)}$$

Where:
$f_{ct,f}$ Tensile strength in bending
F Load
L Length
b width
d effective depth of the section

Figure 7 illustrate the positioning of the beams, immediately before the beginning of the four-point bending tests. A load cell with a maximum capacity of 300 kN was used to apply the loads, and the recording of dates relating to vertical displacements was made by the LVDTs. The loads were applied incrementally by a manual hydraulic pump incrementing 10 kN per step.

Figure 7. Beam with the tests apparatus before start loading.

III. RESULTS AND DISCUSSION

3.1. Technical characteristics of GFRP bars

The results of the tests to determinate the Effective Diameter (ϕ_{ef}) of the GFRP bars used in the research are presented in Table 3.

Table 3. Results of the Effective Diameter determination test

Sample	m_1 (mg)	m_2 (mg)	l_1 (cm)	l_2 (cm)	l_3 (cm)	L_m (mm)	ϕ_{ef} (mm)
1	51,120	26,130	374.9	374.9	374.9	374.90	9.21
2	50,890	26,000	375.7	375.1	375.7	375.50	9.19
3	50,850	25,840	373.4	373.3	373.6	373.43	9.23
4	51,140	25,970	376.1	376.6	376.8	376.50	9.23
5	51,050	25,630	373.1	373.1	373.1	373.10	9.31
Average	-	-	-	-	-	-	**9.23**

Table 4 shows the Elasticity Modulus results after the Chauvenet criterium was used for statistical validation.

Table 4. Results of Tensile Strength and Modulus of Elasticity test

Sample	Elasticity Modulus (GPa)	Load max (kN)	Cross-sectional area (mm^2)	Tension Resistance (MPa)
1	discarded*	73.00	66.98	1,089.9
2	43.53	81.19	66.98	1,212.2
3	43.58	79.08	66.98	1,180.7
4	44.82	76.86	66.98	1,147.5
5	43.48	71.59	66.98	1,068.8
6	45.13	71.07	66.98	1,061.1
7	43.22	71.18	66.98	1,062.7
8	44.98	70.55	66.98	1,053.3
9	45.43	75.87	66.98	1,132.7
10	41.83	68.54	66.98	1,023.3
Average	**44**	-	-	**1,104.7**

* test failured

3.2. Properties of the concrete used

For the casting of the beams three concreting operations were performed on different days. It should be noted, however, that all concreting operations were conducted using the same proportion of material in the concrete mix, ensuring uniform material properties across the different specimens. The results obtained are presented in Table 5.

Table 5. Physical properties of concrete used in the beams

	B 1	B 2	B 3
Compression Resistance – 3 days (MPa)	25.58	20.23	18.02
Compression Resistance – 7 days (MPa)	30.31	25.58	25.19
Elasticity Modulus - E_c (GPa)	31.2	28.43	27.89

3.3. Beam Test

We present here the procedures and results of the theoretical design calculations for the three beam types tested, aiming to ensure the closest possible approximation between the calculated values and the experimentally obtained data. To this end, we chose to disregard the safety factors traditionally adopted in normative projects, both material resistance reduction factors and action amplification factors. Thus, the resistance values adopted in the analyses were those obtained directly from the previously described laboratory tests, ensuring that the analytical model remained faithful to the actual characteristics of the materials used. This approach allows for a more accurate assessment of the correlation between the theoretical behaviour and the observed performance of the beams subjected to bending.

3.3.1. Beam with steel reinforcement (B1)

Steel-reinforced beams were used as “reference” for comparing the structural performance of the GFRP-reinforced beams. The Structural Design of these beams followed the guidelines of [6] considering the technical and geometric parameters previously established in this study. Table 6 presents the results obtained as by Theoretic analyses and by the tests carried out in the beams, this procedure allowed to evaluate of the “degree of adherence” between the adopted models and the real behaviour of the structural elements.

Table 6. Comparison between theoretical and experimental results of type V1 beams

Type	Sample	Load max (kN)	Resistant Moment (kN.m)	Deflection max (mm)	Relation to the average deflections (%)	Failure mode
B1	Theoretical	76.30	22.89	2.60	605%	steel yielding
	1 (B1.1) Experimental	76.48	22.94	18.98		
	2 (B1.2) Experimental	74.48	22.34	12.47		

Figure 8a and 8b shows graphically the results obtained in **B1.1** e **B1.2** experimental tests.

a)

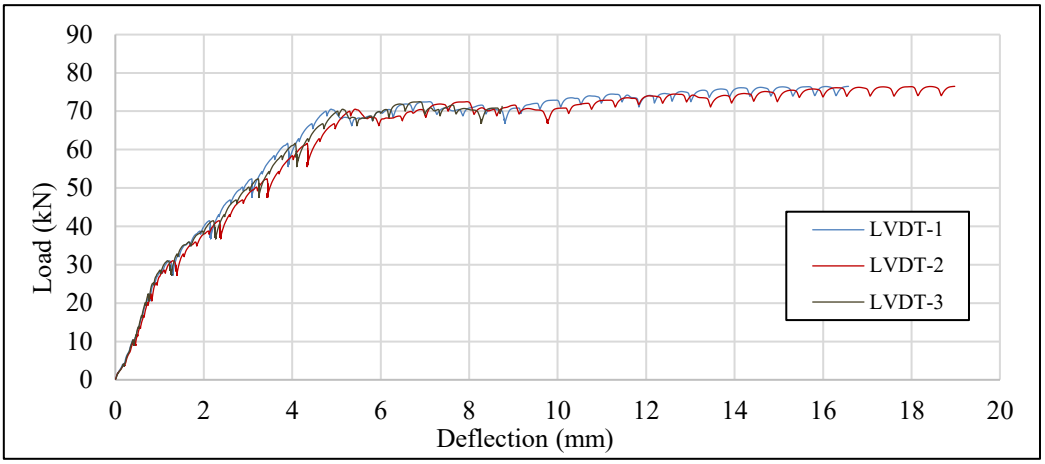

b)

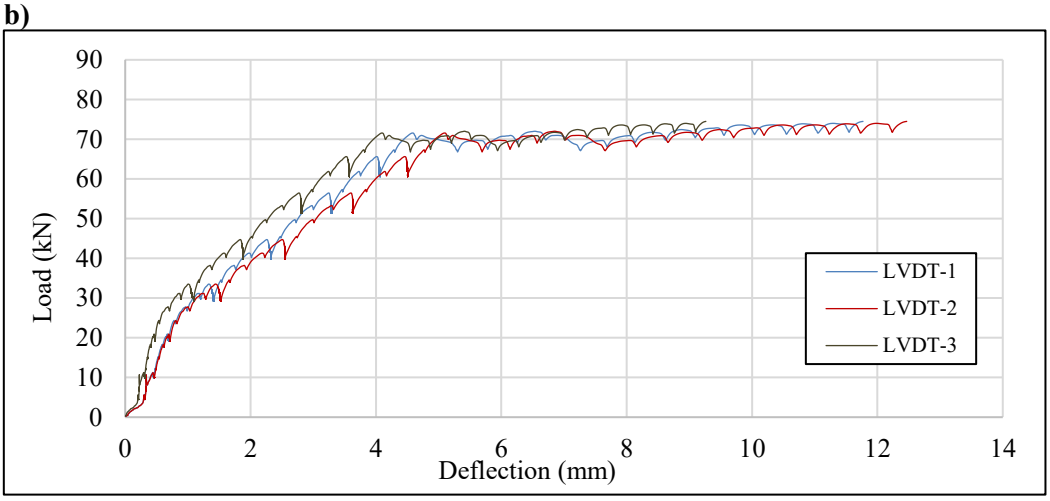

Figure 8. Load vs deflection of beam with steel reinforcement (**B1**). a) **B1.1** and b) **B1.2**

Steel-reinforced beams presented values close to the theoretical estimates. The maximum load of **B1.1** was 0.25% greater than the theoretical estimate, while that of **B1.2** was 2.37% lower. Similarly, the maximum Resistant Moment was 0.25% higher for **B1.1** and **2.37%** lower for **B1.2** compared to the theoretical. The results obtained experimentally presents a considerable difference in relation to theoretical value obtained by Branson's model: beam **B1.1** presented a deflection 630% higher than the theoretic value, and **B1.2** a deflection 380% higher than that calculated theoretically. Therefore, to calculate the theoretical deflection, the estimated radius of curvature of the beam will be derived through deflection, so that, with its equivalent stiffness and its deflection can be calculated from its theoretical data. Table 7 shows the calculation of equivalent stiffness as explained previously.

Table 7. Determination of Equivalent Stiffness of B1

Sample	Load (kN)	Resistant Moment (kN.m)	Radius of curvature (cm)	Equivalent Stiffness (kN.cm²)	Equivalent stiffness at rupture (kN.cm²)
B1.1	30.00	900.00	50,000.00	45,000,000.00	4,726,830
	41.62	1,248.62	25,000.00	31,215,472.70	
	53.24	1,597.24	15,789.40	25,219,426.77	
	64.86	1,945.86	12,162.18	23,665,859.73	
	76.48	2,294.48	1,873.56	4,298,837.76	
B1.2	30.00	900.00	22,222.24	20,000,016.00	

41.12	1,233.62	11,250.03	13,878,302.51
52.24	1,567.25	8,333.37	13,060,450.80
63.36	1,900.87	6,716.46	12,767,122.69
74.48	2,234.49	2,306.93	5,154,822.17

Based on the average stiffness, it was possible to calculate the deflection for the Theoretical Moment value and analysed with the tested deflection of the beams. Table 8 presents these calculations.

Table 8. Calculation of maximum deflection with the stiffness of the Radius of curvature of beam B1

Sample	Load (kN)	Resistant Moment (kN.m)	Maximum Deflection (mm)
Theoretical	76.29	22.89	16.71
1 (**B1.1**) Experimental	76.48	22.94	18.98
2 (**B1.2**) Experimental	74.48	22.34	12.47

With the correction of the Equivalent Stiffness through the Radius of Curvature of the beam. Applying the curvature method dramatically improved the accuracy of the deflection model, reducing the discrepancy from over 600% to approximately 13-25%.

3.3.2. Beam with GFRP reinforcement (B2)

The beam Type 2 (**B2**) was design with GFRP (longitudinal) and can be considered as "super reinforced". The objective of this was to compensate the lower Modulus of Elasticity of GFRP (about 45 GPa) if compared to steel (about 210 GPa) seeking to reduce excessive deformations and improve the overall stiffness of the structural element. By adopting an additional amount of reinforcement, it was sought to ensure that the beam's behaviour under four-point loading would present satisfactory structural performance, both in terms of strength and displacement. Table 9 presents a comparison between the theoretical and experimental values, allowing us to evaluate the effectiveness of the adopted super-reinforcement strategy.

Table 9. Comparison between theoretical and experimental results of **B2** beams.

Type	Sample	Load max (kN)	Resistant Moment (kN.m)	Deflection max (mm)	Relation to the average deflections (%)	Failure mode
B2	Theoretical	137.17	41.15	10.76	252%	Concrete crushing
	1 (**B2.1**) Experimental	137.86	41.36	33.06		shear force
	2 (**B2.2**) Experimental	118.98	35.69	21.22		shear force

Figure 9a and 9b demonstrates graphically the results obtained in the test of beam **B2.1** and **B2.2**.

a)

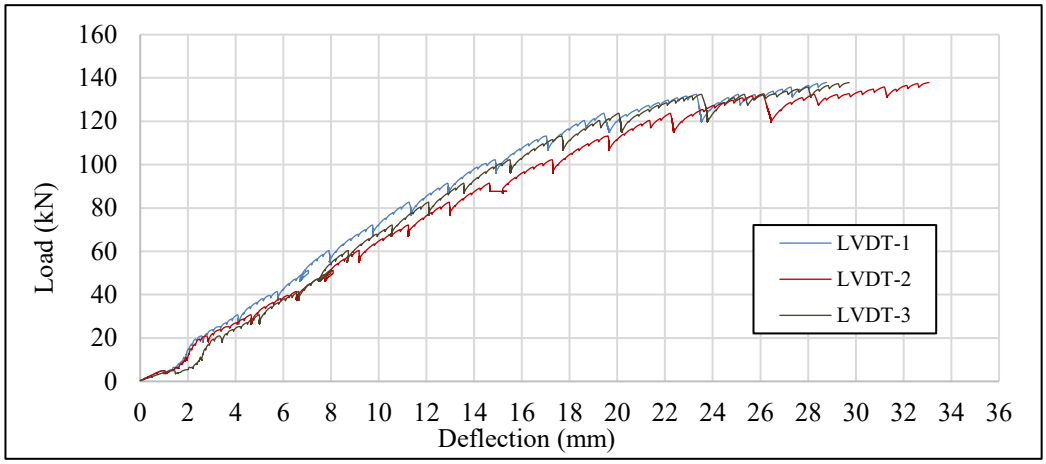

b)

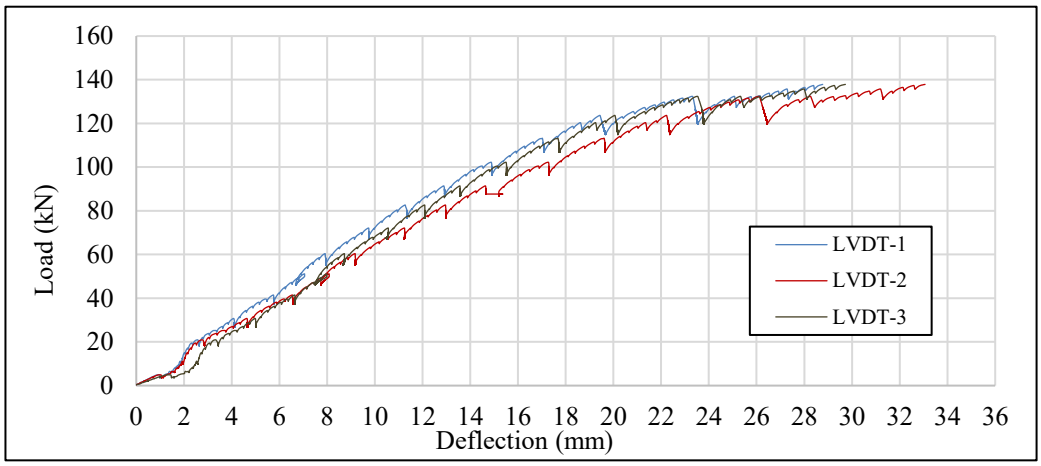

Figure 9. Load vs deflection of beam with GFRP reinforcement (**B2**). a) **B2.1** and b) **B2.2**

The analysis of the results obtained for Type B2 beams, designed with a super reinforcement of GFRP bars, highlights the effects of adopting this strategy on the structural behaviour of the elements. The maximum experimental failure load of beam **B2.1** was 0.50% higher than the estimated theoretical value, while beam **B2.2** performed 13.26% lower than the design prediction. Despite the variation between the results, both beams maintained the failure mode characterized by shear failure, indicating that the actual force transferred to the transverse reinforcement exceeded that predicted in the design. Regarding the deflections, **B2.1** had a deflection 207.36% higher than the theoretically calculated deflection, and beam **B2.2** had a deflection 97.27% higher. Similar to what was done with the steel-reinforced beam, the equivalent stiffness of the two tested beams will be calculated using the radius of curvature of the displacements observed during the test, and Table 10 shows the calculations from this model.

Table 10. Determination of equivalent stiffness B2

Sample	Load (kN)	Resistant Moment (kN.m)	Radius of curvature (cm)	Equivalent Stiffness (kN.cm²)	Equivalent stiffness at rupture (kN.cm²)
B2.1	30.00	900.00	37,500.13	33,750,117.00	5885799,22
	56.97	1,708.95	5,769.29	9,859,428.15	
	83.93	2,517.90	3,448.35	8,682,600.47	
	110.90	3,326.85	1,986.87	6,610,018.46	

	137.86	4,135.80	1,180.10	4,880,657.58
B2.2	30.00	900.00	13,325.31	11,992,779.00
	52.25	1,567.35	5,172.46	8,107,055.18
	74.49	2,234.70	3,435.18	7,676,596.75
	96.74	2,902.05	2,412.96	7,002,530.57
	118.98	3,569.40	1,930.56	6,890,940.86

From the average stiffness it was possible to calculate the deflection for the theoretical moment value and analysed with the tested deflection of the beams, Table 11 exemplifies these calculations.

Table 11. Determination of the maximum deflection with the stiffness of the radius of curvature of the beam B2.

Sample	Load (kN)	Resistant Moment (kN.m)	Maximum Deflection (mm)
Theoretical	137.17	41.15	24.12
1 (B2.1) Experimental	137.86	41.36	33.06
2 (B2.2) Experimental	118.98	35.69	21.22

The model correction was also successful for the GFRP beams, closing the gap between theoretical and experimental deflection from over 200% to within 37%.

3.3.3. Beam with GFRP reinforcement and altered moment of inertia (B3)

The beam Type **B3** was designed using GFRP bars as longitudinal reinforcement but with a change in the cross-section geometry: the height was increased by 5 cm, resulting in dimensions of 15 × 35 x 200 cm. The dimensioning of this element was carried out in accordance with the recommendations of [2] standard. Table 12 shows the predicted theoretical results and the experimental values obtained in the bending tests.

Table 12. Comparison between theoretical and experimental results of type B3 beams

Type	Sample	Load max (kN)	Resistant Moment (kN.m)	Deflection max (mm)	Relation to the average deflections (%)	Failure mode
B3	Theoretic	114.69	34.41	9.69	186%	Concrete crushing
	1 (B3.1)	76.14	22.84	18.54		GFRP bar Rupture
	2 (B3.2)	80.89	24.27	17.52		GFRP bar Rupture

Figure 10 demonstrates the results obtained in the test of beam **B3.1** and **B3.2**, instrumented with LVDTs at three points.

a)

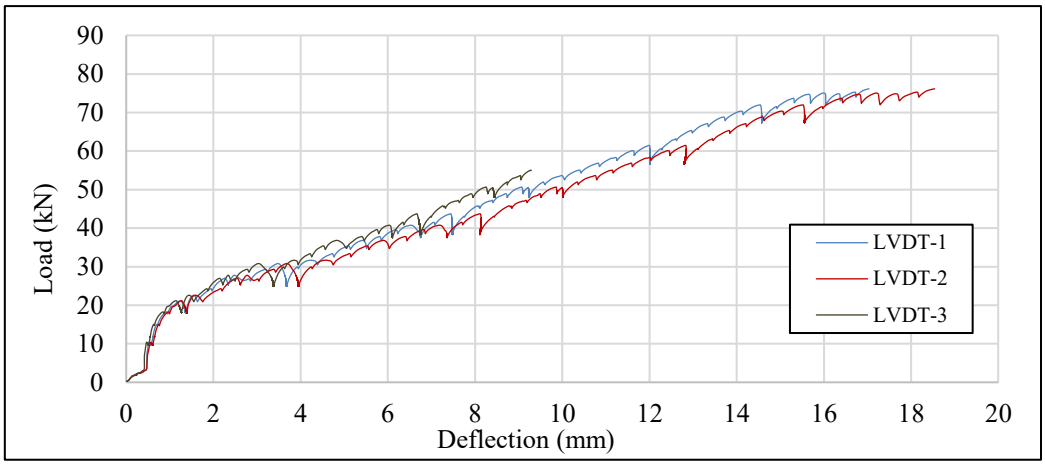

b)

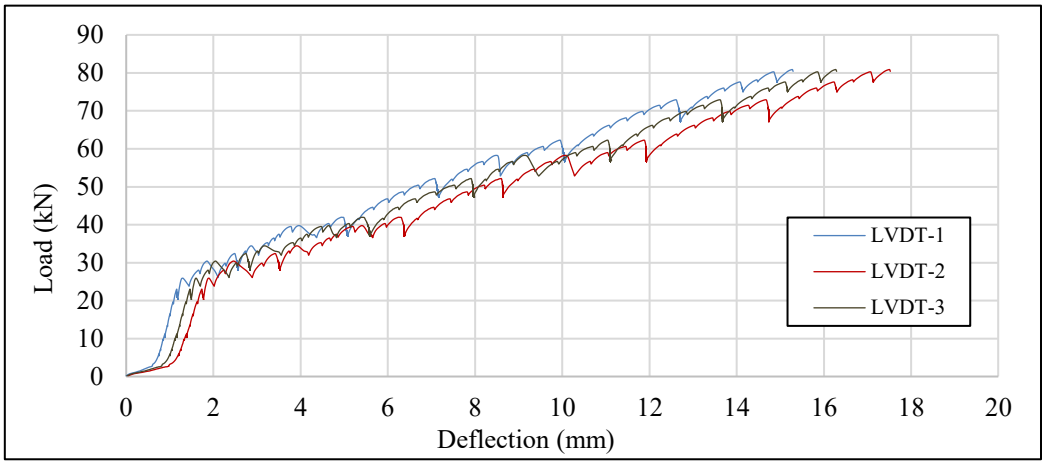

Figure 10. Load vs deflexion of beam with GFRP reinforcement (**B3**). a) **B3.1** and b) **B3.2**

The results obtained for beams type 3 (**B3**), reinforced with GFRP bars and with a modified moment of inertia cross-section, reveal discrepancies between theoretical and experimental values, especially in the type of failure. While the theoretical calculation predicted failure by crushing of the concrete, the experimental tests indicated that both beams failed due to rupture of the longitudinal GFRP bars. This may have been caused by the characteristic brittle behaviour of GFRP, or that the shear force in the stirrups may have cut the GFRP bars. Table 13 shows the shear strength values.

Table 13. Determination of the shear strength of the beam

Sample	Load Max shear (kN)	VRd_2 (kN)	Vc (kN)	Vsw (kN)	VRd_3 (kN)
B3 Theoretic	57.35	292.95	51.69	53.45	105.14
B3.1	38.07				
B3.2	40.45				

Comparing the Load maximum values, **B3.1** presented 33.62% less capacity than the theoretical value, while **B3.2** was 29.47% below the predicted value. The experimental resistant moments followed the same trend, with reductions of 33.62% for **B3.1** and 29.47% for **B3.2** compared to the theoretical calculation. Regarding the deflections, it was observed that both tested beams had deflections greater than the theoretical value calculated according to the Branson model: **B3.1** had 91.36% and **B3.2** had 80.86%. As was done for the other beams, the equivalent stiffness will be calculated using the radius of

curvature of the displacements observed during the test, and Table 14 shows the calculations for this model.

Table 14. Determination of Equivalent Stiffness B3

Sample	Load (kN)	Resistant Moment (kN.m)	Radius of curvature (cm)	Equivalent Stiffness (kN.cm²)	Equivalent stiffness at rupture (kN.cm²)
B3.1	30.00	900.00	9375.03	8,437,527.00	7,150,067.57
	41.54	1,246.05	4522.67	5,635,472.95	
	53.07	1,592.10	3643.80	5,801,293.98	
	64.61	1,938.15	5232.60	10,141,563.69	
	76.14	2,284.20	2601.22	5,941,706.72	
B3.2	30.00	900.00	5389.26	4,850,334.00	
	42.72	1,281.68	4186.11	5,365,232.53	
	55.45	1,663.35	2903.31	4,829,220.69	
	68.17	2,045.03	2903.31	5,937,341.53	
	80.89	2,426.70	3444.36	8,358,428.41	

From the average stiffness, it is possible to calculate the deflection for the theoretical moment value and analysed with the tested deflection of the beams. Table 15 presents these calculations.

Table 15. Determination of the maximum deflection with the stiffness of the radius of curvature of the beam B3.

Sample	Load (kN)	Resistant Moment (kN.m)	Maximum Deflection (mm)
Theoretical	114.69	34.41	16.60
1 (**B3.1**) Experimental	76.14	22.84	18.54
2 (**B3.2**) Experimental	80.89	24.27	17.52

Similarly, for the heightened beam B3, the revised model yielded deflections within 12% of the experimental values.

3.3.4. Synthesis of the beams tests

Table 16 and figure 11 summarize the values obtained in the three types of beams, theoretical and experimental.

Table 16. Synthesis of the results obtained

Sample	Load (kN)	Resistant Moment (kN.m)	Maximum Deflection (mm)	Equivalent stiffness at rupture (kN.cm²)	Failure mode
B1 Theoretical	76.30	22.89	2.63	30,074,525.12	steel yielding
B1 Theoretical*	76.30	22.89	16.71	4,726,829.97	steel yielding
B1.1	76.48	22.94	18.98	4,298,837.76	steel yielding
B1.2	74.48	22.34	12.47	5,154,822.17	steel yielding

B2 Theoretical	137.17	41.15	10.76	13,197,888.78	Concrete crushing
B2 Theoretical*	137.17	41.15	24.12	5,885,799.22	Concrete crushing
B2.1	137.86	33.06	33.06	4,880,657.58	GFRP bar Rupture
B2.2	118.98	21.22	21.22	6,890,940.86	GFRP bar Rupture
B3 Theoretical	114.69	34.41	9.69	12,252,145.45	Concrete crushing
B3 Theoretical*	114.69	34.41	16.60	7,150,067.57	Concrete crushing
B3.1	76.14	18.54	18.54	5,941,706.72	GFRP bar Rupture
B3.2	80.89	17.52	17.52	8,358,428.41	GFRP bar Rupture

* Theoretical calculation made from the equivalent stiffness of the radius of curvature of the beam.

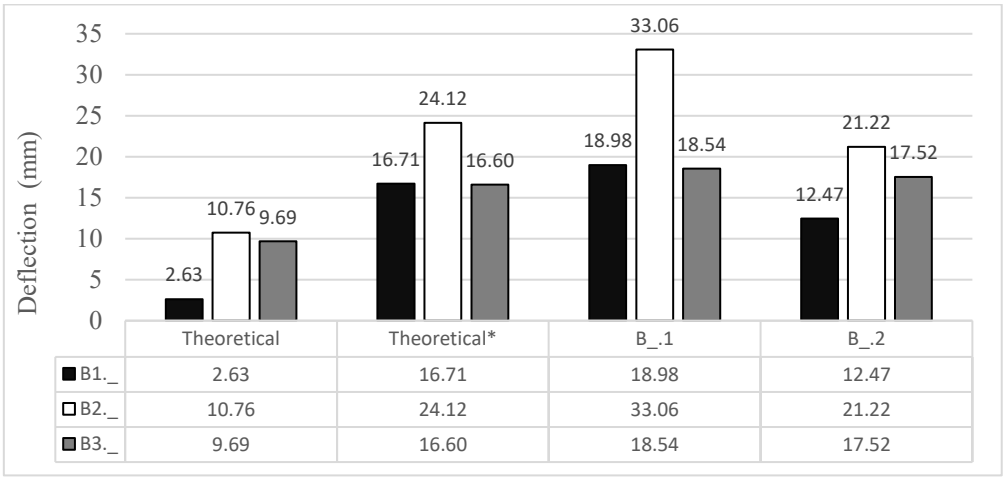

Figure 11. Deflection for each type of beam

To evaluate the efficiency between the three models, an analysis can be carried out based on the Serviceability Limit State Criterion for vertical deformation and observe for the same arrow which of the three models can support better based on the theoretical values and the equivalent stiffness taken from the tests, as shown in Table 17.

Table 17. Comparison between forces for limit deflection

Beam	Load (kN)	Resistant Moment (kN.m)	Maximum Deflection (mm)	Deflection limit L/240 (mm)	F_{max} for Deflection limit (KN)
B1*	76.29	22.89	16.71	7.50	34.25
B2*	137.17	41.15	24.12	7.50	42.65
B3*	114.69	34.41	16.60	7.50	51.81

* Values from Equivalent Inertia.

IV. CONCLUSION

Experimental tests and theoretical analyses showed that GFRP-reinforced beams outperform steel-reinforced beams in Bending Moment performance, supporting up to 80% more load. However, vertical

deformations in GFRP-reinforced beams were significantly greater than in steel-reinforced beams, which exhibited deflections up to 75% greater than those of the steel beam.

The strategy of increasing the beam height to vary the moment of inertia proved highly effective in mitigating excessive deflections, yielding results comparable to the steel-reinforced reference beams, with an 8% reduction in vertical displacement between beams **B1.1** and **B3.2** and a 48% increase between beams **B1.2** and **B3.1**. These results indicate that increasing the cross-section, when possible, is a viable alternative for controlling deformations in concrete structures reinforced with GFRP bars.

Another relevant aspect was the uncertainty associated with the failure mode of GFRP-reinforced beams. Maybe due to the high variability inherent in the material and the adoption of more conservative safety factors compared to steel, in some situations the theoretically predicted failure type differed from that observed experimentally. A notable example was **B**3, whose failure occurred by shear: the steel stirrups cut through the GFRP bars, resulting in a failure load lower than theoretically estimated. Despite these variations in structural behaviour, the use of GFRP remains a viable technical alternative, especially in applications requiring high durability and long service life. As demonstrated in this research, GFRP's high tensile strength ensures adequate levels of structural safety.

ACKNOWLEDGEMENTS

The authors would like to thank FAPEMIG for providing the scholarship and Vergraf Brasil. CSN Cimentos Brasil S.A., Owens Corning and Concrefiber for donating the materials used in this research.

REFERENCES

[1] ISSA. Mohamed S.; METWALLY. Ibrahim M.; ELZEINY. Sherif M. (2011) Influence of fibers on flexural behavior and ductility of concrete beams reinforced with GFRP rebars. Engineering Structures. v. 33. p. 1754–1763. DOI: 10.1016/j.engstruct.2011.02.014.

[2] AMERICAN CONCRETE INSTITUTE (2015) ACI 440. 1R - 15: Guide for the design and construction of structural concrete reinforced with fiber reinforced polymer (FRP) bars. American Concrete Institut.

[3] ASSOCIACAO BRASILEIRA DE NORMAS TECNICAS (2024) NBR 17201-1: Barras de polimero reforcado com fibras (FRP) destinadas a armaduras para estruturas de concreto armado parte 1: Requisitos. Rio de Janeiro.

[4] ASSOCIACAO BRASILEIRA DE NORMAS TECNICAS (2022) NBR 6349:2022. Barras. cordoalhas e fios de aço para armaduras de protensao - Ensaio de tracao. Rio de Janeiro.

[5] ASTM INTERNATIONAL. Standard Test Methods and Definitions for Mechanical Testing of Steel Products, Designation A370-21, ASTM International, West Conshohocken, PA, 2021. DOI: 10.1520/A0370-21.

[6] ASSOCIACAO BRASILEIRA DE NORMAS TECNICAS (2023) NBR 6118: Projeto de estruturas de concreto. Rio de Janeiro.

[7] BISCHOFF, P. (2005) Reevaluation of Deflection Prediction for Concrete Beams Reinforced with Steel and Fiber-Reinforced Polymer Bars. Journal of Structural Engineering. v. 131. p. 752-767.

[8] MOTA, Carlos; ALMINAR, Sandee; SVECOVA, Dagmar (2006) Critical review of deflection formulas for FRP-RC members. Journal of Composites for Construction. v. 10. n. 3. p. 183–194. DOI: 10.1061/(ASCE)1090-0268(2006)10:3(183).

[9] BRANSON. D. E. (1965) Instantaneous and Time-Dependent Deflections of Simple and Continuous Reinforced Concrete Beams. HPR Report n. 7. Alabama Highway Department. Bureau of Public Roads. Montgomery. AL. Part 1. 78p.

[10] CANADIAN STANDARDS ASSOCIATION (CSA) (2002) CSA S806-02: Design and construction of building structures with fibre reinforced polymer (FRP) reinforcement. Mississauga. ON: CSA.

[11] RIBEIRO, Arthur F. Claro; PERUZZI, Antonio P.; MARMORATO GOMES, Carlos E. (2024) Influence of glass and Polypropylene fibers on the residual tensile strengths of hybrid fiber reinforced concrete. International Journal of Advances in Engineering & Technology IJAET. v. 17. n. 6. p. 566-579. DOI: 10.5281/zenodo.14730955.

[12] ASSOCIACAO BRASILEIRA DE NORMAS TECNICAS (2010) NBR 12142:2010 Concreto - Determinação da resistência à tração na flexão de corpos de prova prismáticos. Rio de Janeiro.

Authors

Davi Pitangui P. Abreu graduated in Civil Engineering from the Federal University of Uberlandia (UFU) in 2025. His research interest centers in structural engineering and innovative solutions including the use of GFRP as an alternative to steel reinforcement, aiming for greater durability, corrosion resistance, and efficiency in aggressive environments.

Arthur Francisco Claro Ribeiro. graduated in Civil Engineering from the Federal University of Uberlandia (UFU) in 2022 and master's degree in Civil Engineering at the same university in 2024. His research interests include alternative and sustainable materials for construction. as well as the study of the non-metallic bars (GFRP). and hybridization of glass and polymer fibers to concrete.

Antonio de Paulo Peruzzi. Civil Engineer from University Federal of Sao Carlos (UFScar) in 1997. master's in architecture and Urbanism from the University of Sao Paulo (USP) and Ph.D in Architecture. Urbanism and Technology from the University of Sao Paulo (USP). P.D. in Science and Material Engineering (USP) in light concrete. Works as a professor and researcher at the Faculty of Civil Engineering (FECIV) of the University Federal of Uberlandia (UFU) in fiber-reinforced concrete. non-metallic bars (GFRP) and magnesium oxide-based composites.

Rodrigo Gustavo Delalibera. Graduated in Civil Engineering from the Faculty of Engineering of S Jose do Rio Preto (1999), Master's in Civil Engineering (Structural Engineering) from the University of Sao Paulo (2002), PhD in Civil Engineering (Structural Engineering) from the University of Sao Paulo (2006), and Post-Doctorate in Civil Engineering (Structural Engineering) from the University of Sao Paulo (2009). Currently, he is a Tenured Professor at the Federal University of Uberlandia. He has experience in Civil Engineering, with emphasis on Concrete Structures, mainly working on the following topics: piled foundations, reinforced and prestressed concrete, foundations, numerical and experimental analysis.